Chapter 8

Reconstituting the Motility of Intraflagellar Transport Trains Ex Vivo

Aditya Chhatre, Ludek Stepanek, Stefan Diez and Gaia Pigino

Abstract

Intraflagellar transport (IFT) is essential for the assembly, maintenance and function of most eukaryotic cilia. It acts as a bidirectional cargo transport system, powered by kinesin and dynein motors to navigate through the crowded ciliary environment. Here, we describe a method to isolate intact IFT trains from live cells and reconstitute their motility on synthetic microtubules in vitro. This system enables the controlled investigation of the biophysical properties of IFT trains, including their sensitivity to tubulin post-translational modifications. With minor adaptations, this approach can be extended to study other intracellular transport processes.

Keywords Intraflagellar transport, Kinesin, Dynein, Microtubules, In vitro motility assay, Cilia, Ex vivo single cell assay

1 Introduction

Cilia, also known as flagella, are microtubule-based organelles present on the surface of most eukaryotic cells, where they perform sensory and motility functions. Their internal cytoskeletal scaffold, the axoneme, consists of nine microtubule doublets, each comprising a complete A-tubule and an incomplete B-tubule. Intraflagellar transport (IFT) is a molecular motor-driven system critical for cilia assembly and function [1]. Anterograde IFT trains, powered by kinesin-2, travel along the B-tubules to the ciliary tip, where they unload their cargo and rearrange into dynein-driven retrograde trains, which return to the cell body along the A-tubules [2]. Such complex transport machinery requires precise organization, which remains challenging to study within the intricate environment of a living cell.

Many biochemical and biophysical properties of molecular motor systems can be dissected in vitro under controlled conditions [3],

Supplementary Information The online version contains supplementary material available at https://doi.org/10.1007/978-1-0716-5515-3_8

Noa B. Martín-Cófreces et al. (eds.), *The Cytoskeleton*, Methods in Molecular Biology, vol. 3070,
https://doi.org/10.1007/978-1-0716-5515-3_8,

for example, using techniques such as single molecule stepping assays [4], optical trapping [5], three-dimensional motility assays [6], controlled molecular crowding [7], and exposure to modified microtubules [8]. We sought to reconstitute IFT movement on synthetically polymerized microtubules with defined post-translational modifications to determine whether IFT train motility is influenced by such biochemical cues [9].

In vitro motility assays usually require purification of functional motor complexes in sufficient quantity. However, IFT is an elaborate system, composed of at least 22 different proteins [10], organized into A- and B- complexes [11], which polymerize to form long linear trains [12]. Despite significant progress [13, 14], complete reconstitution of functional IFT trains from purified components has not yet been achieved. We therefore adopted the ex vivo reconstitution approach. While IFT material can be isolated from cilia in bulk [15], its native architecture is not retained during the purification process [16] due to weak interactions between some of its subcomplexes [17]. To overcome this, we developed an assay to transfer intact, motile IFT trains directly from cilia onto synthetic microtubules. Our method leverages several convenient properties of the biflagellate alga *Chlamydomonasreinhardtii*, which we use as a source of IFT trains. A comprehensive range of fluorescently tagged or mutated strains is available for this model organism [18], and additional modifications can be introduced via established protocols [19]. Upon contact with a solid surface, *Chlamydomonas* transitions from swimming to gliding motility, tightly attaching its outstretched cilia to the substrate in a configuration suitable for IFT extraction. Moreover, the *Chlamydomonas* cell body is protected by a detergent-resistant cell wall, while the ciliary membrane is not. This allows selective extraction of the ciliary compartment without lysing the entire cell.

Overview of the reconstitution setup is illustrated in Fig. 1. To deliver intact IFT trains onto synthetic microtubules, living *Chlamydomonas* cells are allowed to glide on a coverslip coated with microtubules. Ciliary membranes are then selectively solubilized using detergent, enabling IFT trains to transfer directly onto the synthetic microtubules after detaching from the axonemal microtubule doublets. Because the gliding cells adhere to the surface via transmembrane proteins [20], strong detergent treatment (when introduced in bulk—using pipetting or microfluidics) can displace both the cell bodies and the released IFT trains before the trains have a chance to rebind. To overcome this issue, we developed a method for locally dispensing femtoliter volumes of detergent using a capillary micropipette. In the presence of ATP-containing motility buffer, some IFT trains detach from the demembranated axonemes and immediately rebind to the synthetic microtubules, where their motility can be observed (Fig. 2a). Some IFT trains do not detach immediately, allowing their motility to be observed on

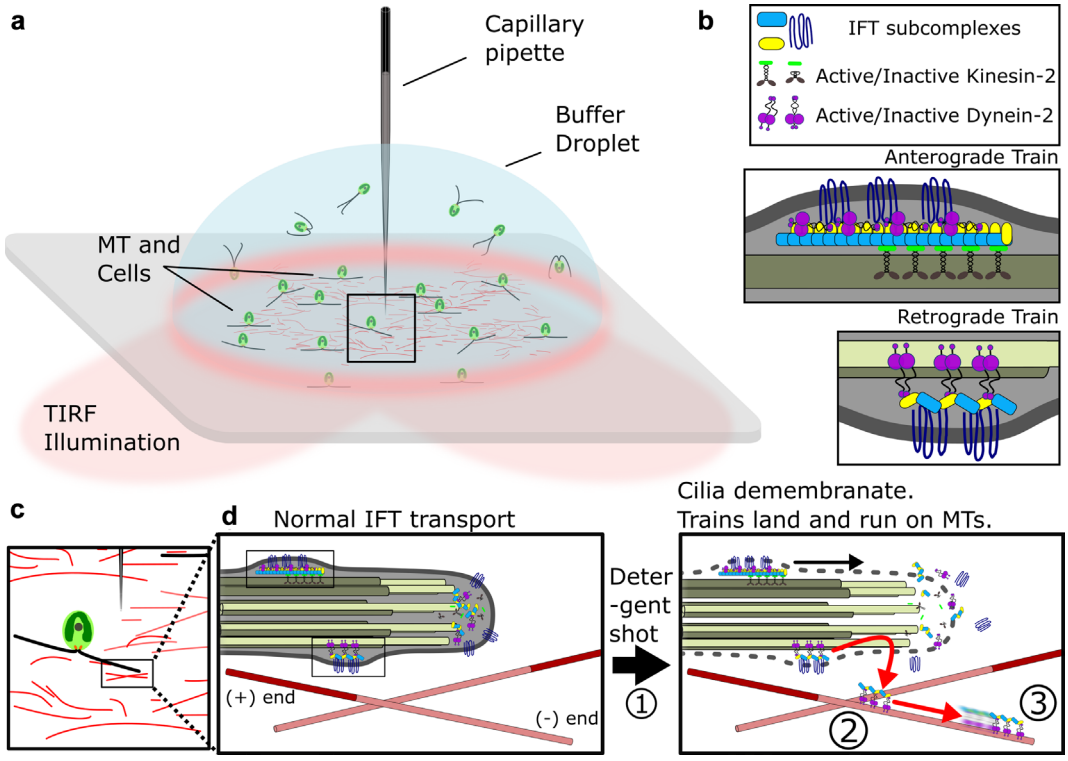

Fig. 1 Overview of IFT train motility reconstitution setup. (**a**) *Chlamydomonas* cells gliding on synthetic microtubules adhered to a coverslip in a droplet of motility buffer on a TIRF microscope. A detergent-filled micropipette is vertically immersed in the buffer. (**b**) Legend showing components of IFT trains (top), and illustrative representations of an anterograde (middle) and retrograde train (bottom). (**c**) Illustration of relative positions of microtubules, cells, and capillary pipette.(**d**) Illustration of in vivo IFT train motility (left) and ex vivo IFT train motility on synthetic polarity-marked microtubules (right). ① Detergent shot from capillary pipette solubilizes ciliary membrane. ② IFT trains are released into the surrounding environment. Some motile trains continue to move (black arrow) on the demembranated cilia (parent axoneme), while ③ others land and move (red arrows) on the polarity-marked microtubules. (Reproduced from ref. [9] under CC BY 4.0)

membrane-free axonemes and enabling quantification of detachment kinetics (Fig. 3). As the detergent diffuses rapidly after ejection, its area of effect is confined to approximately 30 μm (see Fig. 4a, b). This localized treatment enables us to repeat the extraction procedure on neighboring cells within the same sample, significantly improving experimental throughput. The entire procedure is carried out on an inverted microscope, and images are recorded using total internal reflection fluorescence (TIRF) microscopy (see Movie 1). Analysis of the TIRF video sequences reveals that the mean velocity of IFT trains does not change during motility reconstitution (Fig. 2b), suggesting that the IFT architecture and function remain conserved.

In conclusion, we introduce an ex vivo method for reconstituting the motility of intact IFT trains extracted directly from detergent-lyzed cells. Our assay is applicable to any cell type or organism

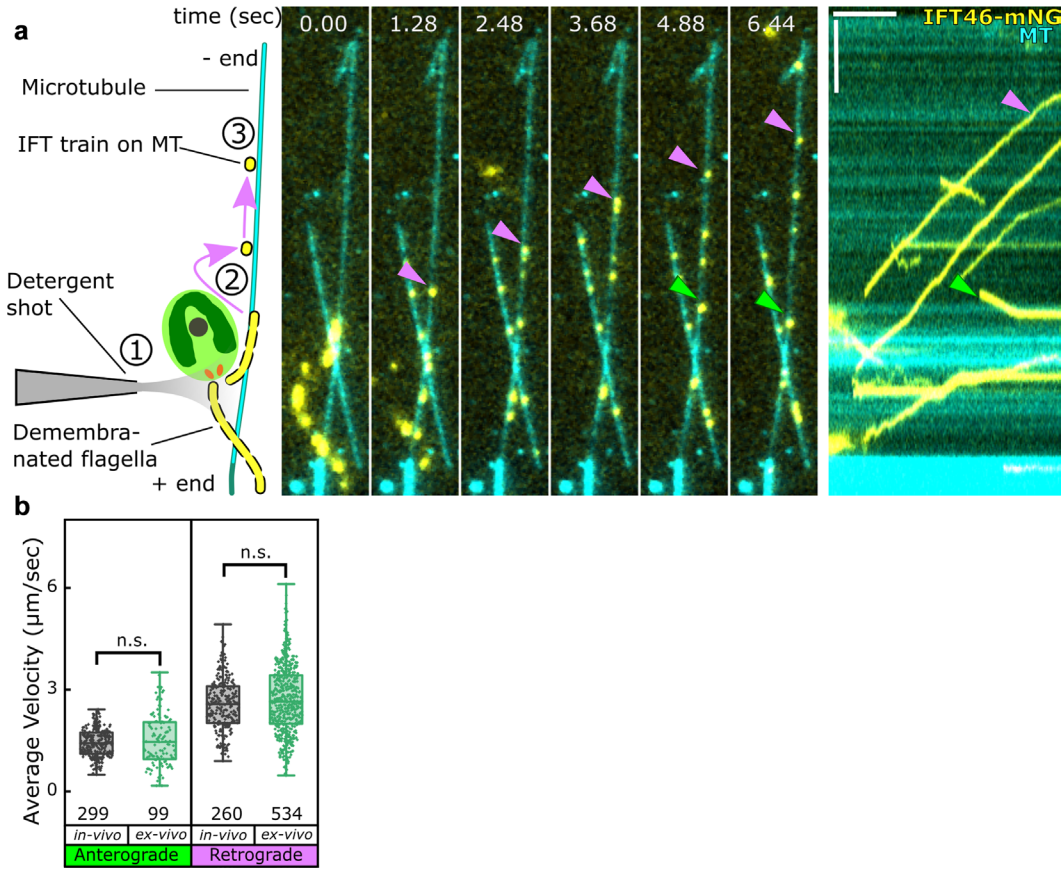

Fig. 2 Observation and analysis if IFT trains during ex vivo motility reconstitution.(**a**) Left: Schematic of ① detergent shot, ② landing of IFT train, and ③ motion on microtubule. Right: Representative time-lapse montage and kymograph of motility reconstitution of IFT trains comprising mNeonGreen labeled IFT46. Timepoint 0.00 shows intact cilia (yellow) attached to synthetic microtubules (cyan). Upon detergent addition, reconstituted anterograde IFT trains (green arrowheads) can be seen moving toward the brightly labeled plus end of a microtubule, while retrograde IFT trains (magenta arrowheads) move toward the minus end. (**b**) Box plots of average velocities as measured from kymographs in (**a**), showing that the velocities of IFT trains remain conserved during motility reconstitution. Statistics by Student's two-tailed *t*-test. n.s., $p =$ not significant. Each point represents an individual train, from 50–70 cells across 6–7 biological replicates. Box bounds represent 25% and 75% quartiles. Line represents the median. Box whiskers represent maxima and minima. Horizontal bar, 5 µm, vertical bar, 2 s. (Adapted from [9] under CC BY 4.0)

that adheres to a coverslip and can be readily implemented in any laboratory with access to TIRF microscope and microinjection instrumentation. In complementary studies, microfluidic platforms have been introduced to analyze single-cell extracts, obtained through mechanical [21] or laser-induced [22, 23] cell disruption. All these targeted ex vivo approaches share several key advantages: they allow rapid reactivation of unstable molecular complexes or transient interactions, capture cell-to-cell variability, minimize input sample

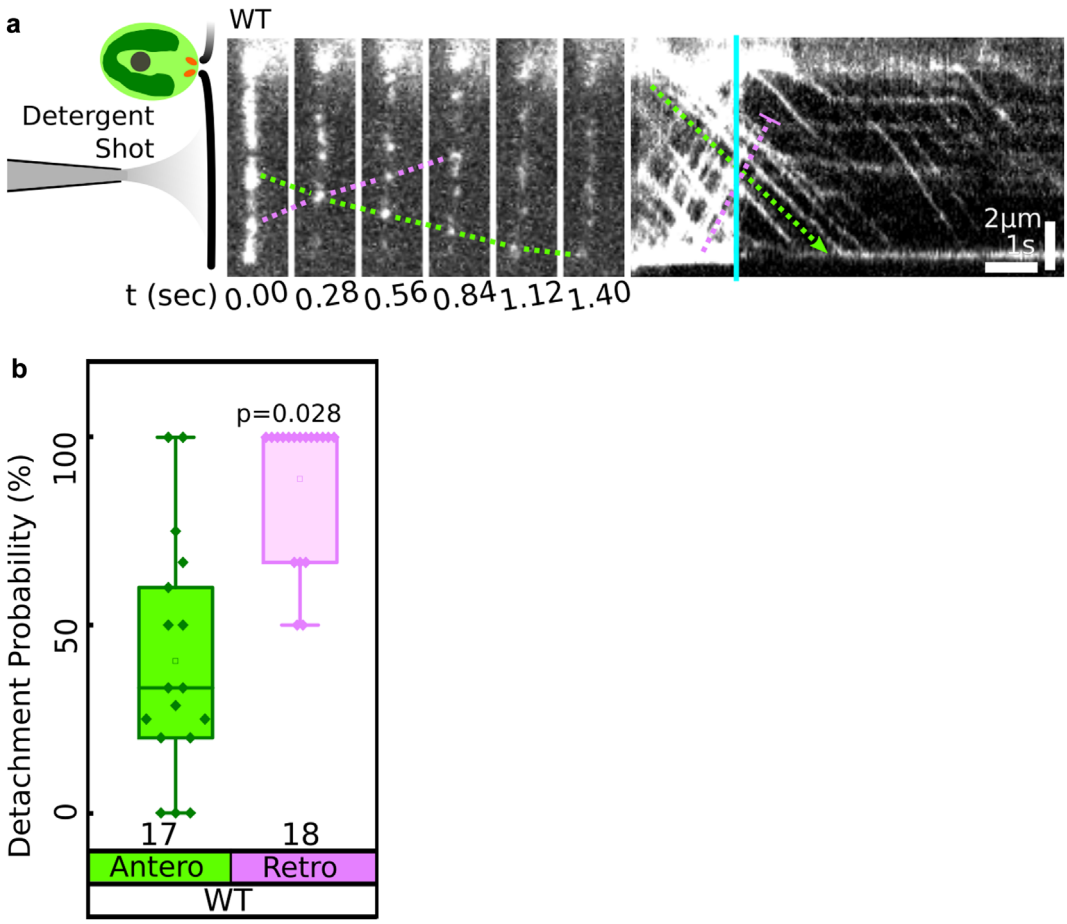

Fig. 3 Observation and analysis of IFT trains detachment from parent axonemes. (**a**) Time lapse montage and kymograph of motility reconstitution of IFT trains comprising mNeonGreen labeled IFT46. Timepoint 0.00 shows intact cilia. Upon detergent addition (cyan line), retrograde train (dashed magenta segment) detaches quickly, while anterograde train (dashed green segment) continues unperturbed to cilia tip. (**b**) Calculated detachment frequency of anterograde or retrograde trains (see Sect. 3.4). Total individual cilia estimated as shown. Statistics by Two-sided Wilcoxon Signed Rank Test. *p*-values as shown. Each point represents an individual axoneme analyzed as shown, from three biological replicates each. Box bounds represent 25% and 75% quartiles. Line represents the median. Box whiskers represent maxima and minima. (Adapted from [9] under CC BY 4.0)

quantity, enable single-molecule sensitivity, and provide immediate experimental readouts. Together, these features facilitate a controlled simplification of the complex and dynamic intracellular environment, offering deeper insight into the organizational principles of living systems.

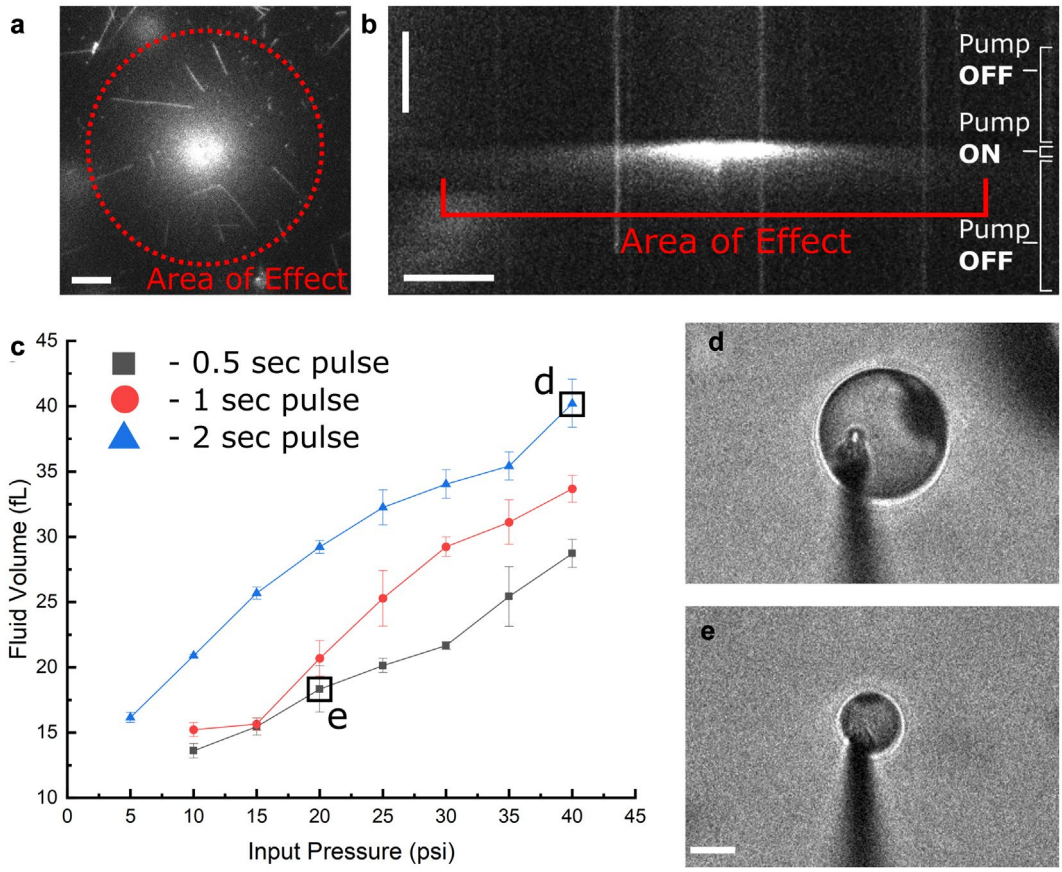

Fig. 4 Calibration of the microinjector pump and capillary pipette. (**a**) Ejection of rhodamine solution to visualize its concentration profile and approximate area of effect across the field of view. Rhodamine-labeled microtubules are present in the field of view. (**b**) Kymograph of ejection dynamics (**c**) Volume of ejected fluid (femtoliter) as a function of pulse duration and input air pressure in the injector pump (psi). Volumes are estimated from radii of fluid spheres. Calibrations were performed across N = 3 repeats, average of 3–4 ejections per data point. (**d, e**) Representative images across the dynamic range of input pressures and pulse times. Horizontal bar, 5 μm, vertical bar, 2 s. (Adapted from [9] under CC BY 4.0)

2 Materials

2.1 Cell Culture

1. *Chlamydomonas* cell line expressing a fluorescently tagged IFT component of choice: several suitable cell lines are available from the Chlamydomonas Resource Center [18].
2. TAP salts: 1.5% NH_4Cl, 0.4% $MgSO_4$, 0.2% KH_2PO_4.
3. Phosphate solution: 28.8% K_2HPO_4, 14.4% KH_2PO_4.
4. Hunter's trace elements stock solution [24], available from the Chlamydomonas Resource Center: 0.134 mM $Na_2EDTA\bullet_2H_2O$, 0.077 mM $ZnSO_4\bullet7H_2O$, 0.184 mM H_3BO_3,

0.026 mM $MnCl_2 \bullet 4H_2O$, 0.018 mM $FeSO_4 \bullet 7H_2O$, 0.007 mM $CoCl_2 \bullet 6H_2O$, 0.005 mM $CuSO_4 \bullet 5H_2O$, 0.0008 mM $(NH_4)_6 Mo_7O_{24} \bullet 4H_2O$.

5. TAP (Tris-Acetate-Phosphate) medium [25]: 0.02 M Trisma Base pH 7, 0.017 M CH_3COOH, 2.5% TAP salts (v/v), 0.1% Phosphate solution (v/v), 0.1% Hutner's trace elements stock solution (v/v) (*see* **Note 1**).
6. Culture cells in bottles aerated with sterile air under 12 h light/12 h dark cycles at 23°C.

2.2 Silanized Coverslips

1. Clean the coverslips (22 × 22 mm, #1.5 thickness coverslips) by 15 min sonication in 5% Mucasol diluted in water.
2. Rinse for 2 min with deionized water.
3. Incubate in 0.05% dichlorodimethylsilane diluted in 90% ethanol/10% methanol (v/v) for 60 min.
4. Rinse and sonicate 2 × 10 min with 100% methanol.
5. Sonicate 2× with deionized water.
6. Blow dry using nitrogen gas.
7. Store in an airtight container.

2.3 Capillary Micropipettes

1. Glass capillaries: borosilicate glass, with filament, thin wall, 1 mm outer diameter (e.g., BF100-75-15, Sutter Instruments).
2. Programmable pipette puller (e.g., P97 or P1000, Sutter Instruments).
3. Optimize the puller settings per manufacturer's instructions (*see* **Note 2**) to obtain suitable pipette parameters of 6–8 mm taper length and 2–3 μm tip size.
4. Inspect micropipettes using a low-magnification stereomicroscope. Pipette shoulders should not have significant asymmetries as this might cause inconsistencies in ejection volumes.
5. Confirm that pipettes dispense consistent liquid volumes in the range of 20–40 fL by using a pipette for injection pump calibration (see Sect. 2.7, Fig. 4).
6. Prepare a batch of 15–20 capillary micropipettes (length 20–40 mm).

2.4 Polarity-Marked Microtubules

To visualize the directionality of reconstituted IFT trains, synthetic microtubules are assembled with brightly labeled plus-ends. This is achieved by extending dim rhodamine labeled microtubule seeds with an elongation mix containing bright rhodamine labeled tubulin. Targeted labeling at the plus-end is ensured through N-ethylmaleimide modification of bright rhodamine tubulin.

1. Unlabeled tubulin: commercially available or purified from porcine brain [26].
2. Rhodamine-labeled tubulin: commercially available or labeled according to standard procedures [27].
3. BRB80 buffer: 80 mM PIPES, 1 mM $MgCl_2$, 1 mM EGTA, pH 6.8.
4. Dimly-labeled microtubule seeds: mix one part of rhodamine-labeled tubulin with nine parts of unlabeled tubulin for a final concentration 2 μM in BRB80, add GMPCPP to 1 mM, and incubate at 37°C for 30 min.
5. N-ethylmaleimide (NEM) tubulin: incubate 40 μM unlabeled tubulin with 0.4 mM NEM on ice for 10 min, and quench excess NEM with 20 mM DTT for 10 min. Use immediately.
6. Plus-end labeling mix: mix one part of rhodamine-labeled tubulin with three parts of unlabeled tubulin for a final concentration of 4 μM, 1 μM NEM-tubulin, 1 mM GTP, 4 mM $MgCl_2$ in BRB80. Prepare on ice.
7. Plus-end labeled microtubules: Warm the plus-end labeling mix at 37°C for 1 min, incubate with 1/10 volume of dimly-labeled microtubule seeds at 37°C for 60 min and stabilize by adding taxol to 10 μM. Harvest by spinning at 17,000 g for 15 min. Polarity-marked microtubules should be used on the same day.

2.5 Instrumentation for Reconstitution and Microscopy: TIRF Microscope

We have successfully validated the procedure using different models of microscopes, micromanipulator and microinjection pumps. For each instrument, we list the key features, followed by the specifications of our typical setup. The TIRF microscope must be configured for high-speed imaging of IFT moving along polarity-marked microtubules. Some features, such as motorized control and automatic focus compensation are beneficial, but not strictly necessary (*see* **Note 3**). Essential features are:

1. Single-molecule detection sensitivity.
2. ≥25 fps frame rate.
3. Simultaneous dual-color imaging.
4. Inverted stand with sufficient space on the sample side to allow micromanipulation. In particular, the condenser arm should be retractable to a sufficient degree. An enclosure box is generally not suitable.

2.6 Instrumentation for Reconstitution and Microscopy: Micromanipulator

The micromanipulator is required to hold the micropipette directly above the objective, in the center of the field of view. Distinct from typical microinjection setups, the pipette is held vertically, not

obliquely (*see* **Note 4**). The following considerations are essential when choosing and installing the micromanipulator (*see* **Note 5**):

1. Coarse positioning in the range of centimeters and fine positioning with precision of 1 μm or smaller in X, Y, Z.
2. Fine positioning should be remotely controlled, electronic or hydraulic.
3. Custom mounting accessories might be needed to install the micromanipulator onto the microscope. Minimize mechanical loop to reduce micropipette vibrations.
4. Ensure that the manipulator cables or connectors do not hinder the objective or optical path in any way.
5. As the micromanipulator usually interferes with the condenser and the transmitted light path, it should be easily detachable from the microscope.

2.7 Instrumentation for Reconstitution and Microscopy: Microinjection Pump

The microinjection pump is used for femtoliter-scale delivery of detergent solution onto the sample. The adjustability of the following settings is essential (*see* **Note 6**):

1. Compensation pressure.
2. Ejection pressure.
3. Ejection pulse duration.
4. To calibrate ejection pressure and ejection pulse duration, inject the demembranation solution (see Sect. 2.8, Step 3) into a droplet of paraffin oil (Fig. 4c–e). Ejected volume can be calculated from the radius of the ejected droplet. Desired volume is 20–40 fL.
5. To validate the setup, eject rhodamine solution into HMDEK solution and observe the pulse kinetics using TIRF microscope. Visible rhodamine fluorescence should encompass an area of approximately 30 μm (Fig. 4a) and dissipate within approximately 1 s (Fig. 4b).

2.8 Reconstitution

1. HMDEK buffer: 30 mM HEPES, 5 mM $MgSO_4$, 1 mM DTT, 0.5 mM EGTA, 25 mM KCl, pH 7.2.
2. Mg^{2+}-ATP solution (100 mM stock).
3. Demembranation solution: 1% Igepal CA-630 (NP-40) detergent in HMDEK.
4. Teflon-tipped tweezers for coverslip handling.
5. Coverslip holder with screw clamps.
6. 1 mL Luer-Lock syringe with 27-gauge beveled needle.

3 Methods

3.1 Preparation of Cells and Microtubules

1. 3–4 days prior to the experiment, inoculate 100–250 mL of TAP medium with the *Chlamydomonas* cell strain of choice.
2. On the day of the experiment, check the cell culture quality: cell suspension should appear bright green and most cells should be swimming when examined with a microscope. Enough cells should adhere to solid surfaces in a gliding position.
3. Prepare polarity-marked microtubules and evaluate their density and labeling quality using a TIRF microscope. Repeat the preparation if microtubule density is low or polarity labeling is inadequate.
4. Aspirate 1–2 mL of the cell suspension from culture bottle (*see* **Note 7**).
5. Wash the cells thrice in HMDEK buffer.
6. Resuspend cells in 1 mL of HMDEK to a final concentration of approximately 10^6–10^7 cells/mL (*see* **Note 8**).
7. Add ATP to the cell suspension to have a concentration of 1 mM in the final cell-microtubule mix. Take into account the volume of microtubule suspension added later (see Sect. 3.2, Step 12; *see* **Note 9**).
8. Keep the suspension on a slow rocker until use.

3.2 Setting Up the Microscope

1. Mount the micromanipulator on the microscope stage so that the pipette holder is perpendicular to the stage and directly above the objective (see Fig. 5).
2. Ensure that manipulator adjustment screws are near the center of their travel range before starting the experiment.
3. Mount a silanized coverslip in the coverslip holder. Avoid over tightening of the holder screws to prevent bending the coverslip.
4. Place the mount on the microscope stage.
5. Fill a syringe with approximately 0.5 mL of demembranation solution.
6. Backfill carefully a capillary micropipette with a few microliters of the demembranation solution by using a 27-gauge needle (*see* **Note 10**).
7. Ensure the solution reaches the tip of the pipette. This can be verified by observing a small meniscus around the pipette shoulder (*see* **Note 11**).
8. Immediately mount it in the pipette holder supplied with the microinjection pump (*see* **Note 12**).

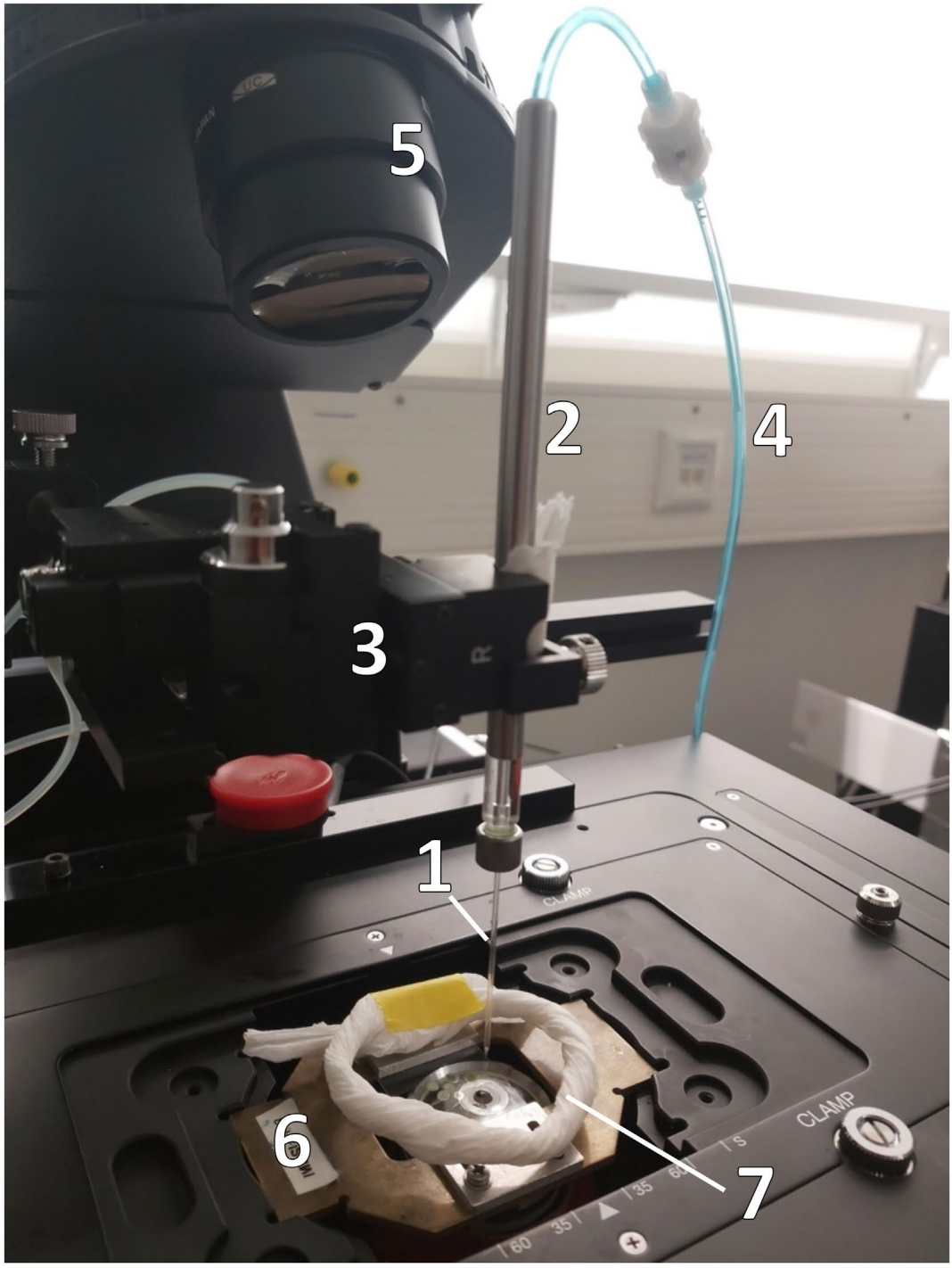

Fig. 5 IFT train motility reconstitution setup mounted on a microscope stage. A capillary micropipette **(1)** inserted in a microinjection pipette holder **(2)**, held vertically by a hydraulic micromanipulator **(3)**, connected to a microinjection pump by tubing **(4)**. Transmitted illumination arm of the microscope **(5)** is retracted back to accommodate the assembly. Coverslip with the sample is mounted in a custom holder **(6)** and surrounded with a wet filter paper **(7)** to reduce evaporation (Reproduced from [28])

9. Mount the pipette holder in the micromanipulator so that the pipette tip is suspended 3–4 cm above the coverslip. Achieve this height by slowly sliding the pipette holder in the manipulator, not by moving the manipulator Z-axis screw (*see* **Note 13**).
10. Start a live video stream at 10× magnification. Turn on the transmitted lamp to illuminate the stage and the pipette tip.
11. Using the coarse manipulator, position the pipette tip directly over the objective. Coarse alignment can be performed looking at the pipette tip from sides (*see* **Note 14**).
12. Once it is approximately centered, slowly lower the pipette using the coarse or fine Z-axis screw (*see* **Note 15**).
13. The pipette tip or its shadow should now appear in the microscope field of view (FOV). Center it using the manipulator coarse X and Y adjustment screws.
14. Raise or lower the tip so that it just touches the surface (*see* **Note 16**). The final tip position should be 10–20 μm above the coverslip, or roughly 1–2 Chlamydomonas cell diameters.
15. Switch to an intermediate magnification objective (40× or 60×).
16. Recenter the pipette.
17. Switch to the TIRF objective (100× or 150×) and repeat the centering (*see* **Note 17**).
18. Place a small droplet (0.5–1 μL) of polarity-marked microtubules on the coverslip a few mm away from the pipette and overlay it slowly with 5–10 μL of the cell suspension in HMDEK-ATP buffer. The final ATP concentration should be 1 mM.
19. Bring the droplet into the FOV so that the pipette tip is immersed and approximately centered (*see* **Note 18**).
20. Recenter the pipette as needed.
21. Check for leakage of liquid from the pipette tip. If necessary, eliminate it by adjusting the compensation pressure on the pump.

3.3 IFT Train Motility Reconstitution on Synthetic Microtubules

1. Turn off the transmitted illumination. Focus the microtubules, cilia and IFT in TIRF mode.
2. Start a continuous video stream recording of 4–5 min duration.
3. Navigate to a field of view (FOV) with a suitable density of microtubules and ciliated cells. FOV of 50 μm × 50 μm containing 6–7 cilia is usually ideal for observing processive IFT runs (*see* **Note 19**).

4. Center the region of interest in the FOV.
5. Trigger the pump to eject a predetermined volume of detergent. The gliding cells will typically detach from the coverslip and begin ciliary motion, as the axonemal motility gets reconstituted along with IFT upon cilia demembranation.
6. Observe IFT trains as they land and move along polarity-marked microtubules.
7. Continue imaging on the same FOV for 3–5 s after demembranation to capture complete runs (see Movie 1).
8. While still imaging, move to a new FOV nearby.
9. Repeat Steps 3–8 until the stream acquisition finishes. The result is a long movie that shows multiple reconstitution events interleaved with segments showing the process of locating and focusing on the next area of interest (*see* **Note 20**).
10. Start over from Step 2 to acquire additional data.
11. Intermittently turn on transmitted light to check the pipette tip remains centered. If off-center or lost from FOV, repeat Steps 9–11, Sect. 3.2, before resuming.
12. Continue recording until the pipette becomes clogged (*see* **Note 21**) or the cells start dying (*see* **Note 22**).
13. Stop recording and begin with a new pipette and fresh cells at that point.
14. At the end of the session, raise the pipette, remove it from the holder, and discard it carefully with sharp waste (*see* **Note 23**).
15. Extract successful reconstitution events from the continuous recordings for further analysis in image analysis software such as FIJI/ImageJ [29]. For a typical analysis, see Fig. 2.

3.4 IFT Train Motility Reconstitution on Parent Axonemes

In addition to studying IFTmotility on reconstituted microtubules, it can also be reconstituted directly on demembraneted axonemes. This approach lets us assess IFT train behavior without interference from the flagellar membrane or cytoplasm. Further, measurement of detachment kinetics after demembranation reveals relative train affinity for the axoneme in-situ, which are illustrated in Fig. 3. These measurements are especially interesting for investigating how microtubule post-translational modifications, associated MAPs, or lattice defects in the microtubule doublets affect IFT motor binding and dynamics. IFT can be reconstituted on parent axoneme with few modifications of the protocol described above.

1. Completely exclude polymerized microtubules for this experiment, as the acquisition will focus on parent axonemes, i.e.,

demembranated axonemes from the cells that are exposed to detergent.

2. Start a continuous video stream recording of 4–5 min duration. Acquire a few seconds of normal in-vivo IFTmotility.
3. Proceed as for Steps 3–14 described in Sect. 3.3.
4. For analysis, include predemembranation frames to be able to efficiently trace back trains later during the analysis.
5. Calculation of Detachment Probability: For each train type on each parent axoneme, calculate "Retention fraction" (Rf) as,
6. $Rf = Npa/Nc$
7. where,
8. Npa = Number of trains per demembranated parent axoneme
9. Nc = Number of trains per cilium before demembranation
10. Disregarding newly injecting trains after demembranation (particularly anterograde trains) in the above evaluation, calculate Detachment Probability as,
11. $Pd = (1 - Rf) \times 100$
12. Occasionally, the target cilium will change shape upon demembranation, due to non-native activation of axonemal dyneins. Trace and plot kymographs individually for each of these shapes during post-processing before taking a maximum Z-projection to obtain full temporal coverage (*see* **Note 24**).

4 Notes

1. Dissolve 2.42 g Tris base in 850 mL of deionized water. Add 25 mL of TAP salts. Add 1 mL of Phosphate solution. Add 1 mL of Hutner's trace elements [24]. Adjust pH to 7.0 using about 1 mL glacial acetic acid. Bring volume to 1 L with deionized water. Autoclave and store at room temperature.
2. Micropipette puller settings must be determined individually for each machine. For consistent results, adjustments may be necessary over time, particularly after replacing the heating filament. Always aim for pipettes with reasonable neck flexibility: rigid neck will shatter upon even light contact with a glass coverslip, while overly flexible neck will be deflected by the surface tension of the sample droplet and thus difficult to center.
3. The setup used in the method described here is: Ti2 Eclipse (Nikon, Japan) equipped with a 100×/1.49NA TIRF

objective with a galvo-driven orbital TIRF (iLas2, Gataca Systems, France) coupled to a multilaser combiner (VSLMS-MOT100, Visitron Systems, Germany). Multicolor, simultaneous acquisition is done with EMCCD cameras (iXon life, Oxford Instruments, UK) controlled by VisiView software 5.0 (Visitron Systems, Germany). Data are acquired as a continuous stream at 40 ms/frame, 1024 × 1024 pixels at a resolution of 0.086 μm/px.

4. Pipettes positioned at non-perpendicular angles allow the manipulator assembly to occupy less headspace over the stage. However, ejecting detergent at an obtuse angle can induce lateral flows, potentially displacing microtubules and reconstituted particles from the field of view (FOV).
5. We used MN-4 for coarse manipulation and MMO-4 for fine manipulation, both Narishige, Japan.
6. Our pump model: PV-850, World Precision Instruments, UK.
7. When using non-hatching *Chlamydomonas* mutants, aspirate the desired quantity and treat with autolysin for 30 min, and allow recovery in fresh TAP for 1–2 h prior to proceeding further.
8. Precise cell concentration matters less for this experiment. However, the number of cells adhered to the glass surface within each TIRF FOV during reconstitution is essential. This may depend on different factors, including the cell strain used, precise stage of the cell cycle, or surface modification of the coverslip.
9. For example, if 0.5 μL of the microtubule suspension is to be overlaid with 5 μL of the cell suspension, add 11 μL of 100 mM ATP to 989 μL of the cell suspension to have an intermediate concentration of 1.1 mM.
10. One microliter of detergent solution is sufficient for a full experiment. Typical ejection volumes are in the femtoliter range.
11. Sometimes the solution may not reach the pipette tip. If this occurs, gently tap the broad end or rub it with a small piece of paper to create frictional vibrations. This should help draw the solution down to the narrow tip.
12. Avoid carrying the pipette around after filling.
13. It is essential to keep the micromanipulator adjustment screws around the middle of their travel range during the preparatory phase. Their travel range is limited and reaching end stops during an experiment leads to tedious realignment.

14. Insufficient headspace over the microscope may prevent the manipulator from fitting when the condenser illumination arm is in proper position. In such cases, illuminate the stage while the condenser arm is retracted. Although this will result in oblique transmitted illumination, it should suffice for locating cells on the surface and centering the pipette tip.
15. Be careful! Do not lower it too quickly or too far. Doing either will break the tip against the coverslip.
16. A good way to confirm contact with the coverslip surface is to observe a slight buckling of the pipette shaft as it touches the glass surface.
17. Pre-emptively raise the pipette during centering to prevent it from breaking or scratching the coverslip. Lower it in a controlled manner using coarse Z-axis adjustment screws. This precaution might be especially important when using high-magnification oil-immersion objectives that physically contact the coverslip. Ensure objectives are not raised so high that they push the coverslip into the pipette tip.
18. Ensure that the pipette tip is fully immersed and not deflected sideways. Sideward deflection can result from interactions between the pipette neck and the surface of the hemispherical liquid drop. If this occurs frequently, the pipette neck may be too flexible and the puller program may require optimization to produce stiffer pipettes.
19. Gliding *Chlamydomonas* cells and microtubule density must be optimized according to experimental needs. Low microtubule density reduces the frequency of reconstituted IFT train runs. Very high density increases run frequency, but complicates tracking due to overlapping and crossing of trajectories.
20. This approach is more efficient than attempting to record only the reconstitution events, as switching between live mode and acquisition can take several seconds. Avoiding these interruptions not only streamlines the experimental workflow but also helps minimize phototoxic damage to the sample. Events of interest are later identified and extracted from the full recording.
21. After prolonged use, debris may accumulate and clog the pipette tip. Keep a small (5–6 μL) droplet of HMDEK buffer or distilled water for washing pipette tip next to the cell suspension, gently move the pipette back and forth within the cleaning droplet using fine adjustment screws to dislodge any contaminants. Discard the pipette if the issue is not resolved and restart the protocol with a new pipette.
22. Over time, repeated detergent ejections and buffer evaporation may reduce cell viability. Placing a small open humidity

chamber over the coverslip (see Fig. 5**,** Sect. 7) can reduce evaporation, although it may also limit the space available for pipette manipulation.

23. Always use a new pipette for each session.
24. In a few cases, especially at saturating ATP concentrations, demembranated cilium will beat and cause whole cell movement, making further analysis impossible. To overcome this, adapt the protocol to immobilize cells further by either lowering ATP concentration in final buffer or choosing a mutant with immobile cilium and an IFT reporter, such as *pf18::*d1bLIC-GFP (CC-4489 in Chlamydomonas Resource Center).

Acknowledgments

We acknowledge all members of the Pigino and Diez labs for fruitful discussions. The project was supported by the Deutsche Forschungsgemeinschaft (DFG, German Research Foundation) under Germany's Excellence Strategy—EXC 2068—390729961 Cluster of Excellence, Physics of Life of TU Dresden (starting grant to A.C.). A.C. and S.D. were further supported by the TU Dresden. L.S. was supported by the INTER-ACTION grant LUAUS24182 by the Czech Ministry of Education, Youth and Sports. G.P. was supported by the Human Technopole, Milan, Italy.

References

1. Kozminski KG, Johnson KA, Forscher P, Rosenbaum JL (1993) A motility in the eukaryotic flagellum unrelated to flagellar beating. Proc Natl Acad Sci USA 90:5519–5523. https://doi.org/10.1073/pnas.90.12.5519
2. Stepanek L, Pigino G (2016) Microtubule doublets are double-track railways for intraflagellar transport trains. Science 352:721–724. https://doi.org/10.1126/science.aaf4594
3. Howard J, Hudspeth AJ, Vale RD (1989) Movement of microtubules by single kinesin molecules. Nature 342:154–158. https://doi.org/10.1038/342154a0
4. Vale RD, Funatsu T, Pierce DW et al (1996) Direct observation of single kinesin molecules moving along microtubules. Nature 380:451–453. https://doi.org/10.1038/380451a0
5. Neuman KC, Nagy A (2008) Single-molecule force spectroscopy: optical tweezers, magnetic tweezers and atomic force microscopy. Nat Methods 5:491–505. https://doi.org/10.1038/nmeth.1218
6. Mitra A, Meißner L, Gandhimathi R et al (2020) Kinesin-14 motors drive a right-handed helical motion of antiparallel microtubules around each other. Nat Commun 11: 2565. https://doi.org/10.1038/s41467-020-16328-z
7. Leduc C, Padberg-Gehle K, Varga V et al (2012) Molecular crowding creates traffic jams of kinesin motors on microtubules. Proc Natl Acad Sci 109:6100–6105. https://doi.org/10.1073/pnas.1107281109
8. Vemu A, Garnham CP, Lee D-Y, Roll-Mecak A (2014) Generation of differentially modified microtubules using in vitro enzymatic approaches. In: Vale RD (Ed.)Eds. Methods in enzymology. Academic Press, 149–166
9. Chhatre A, Stepanek L, Nievergelt AP et al (2025) Tubulin tyrosination/detyrosination regulate the affinity and sorting of intraflagellar transport trains on axonemal microtubule doublets. Nat Commun 16: 1055. https://doi.org/10.1038/s41467-025-56098-0

10. Taschner M, Lorentzen E (2016) The intraflagellar transport machinery. Cold Spring Harb Perspect Biol 8:a028092. https://doi.org/10.1101/cshperspect.a028092
11. Lacey SE, Foster HE, Pigino G (2023) The molecular structure of IFT-A and IFT-B in anterograde intraflagellar transport trains. Nat Struct Mol Biol 30:584–593. https://doi.org/10.1038/s41594-022-00905-5
12. Jordan MA, Diener DR, Stepanek L, Pigino G (2018) The cryo-EM structure of intraflagellar transport trains reveals how dynein is inactivated to ensure unidirectional anterograde movement in cilia. Nat Cell Biol 20:1250–1255. https://doi.org/10.1038/s41556-018-0213-1
13. Taschner M, Lorentzen E (2016) Recombinant reconstitution and purification of the IFT-B Core Complex from Chlamydomonas reinhardtii. In: Satir P, Christensen ST (Eds.)Eds. Cilia: methods and protocols. Springer, New York, NY, 69–82
14. Mohamed MAA, Stepp WL, Ökten Z (2018) Reconstitution reveals motor activation for intraflagellar transport. Nature 557:387–391. https://doi.org/10.1038/s41586-018-0105-3
15. Sloboda RD (2016) Purification and localization of intraflagellar transport particles and polypeptides. In: Gavin RH (Ed.)Eds. Cytoskeleton methods and protocols: methods and protocols. Springer, New York, NY, 119–137
16. Mencarelli C, Mitchell A, Leoncini R et al (2013) Isolation of intraflagellar transport trains. Cytoskeleton 70:439–452. https://doi.org/10.1002/cm.21121
17. Petriman NA, Loureiro-López M, Taschner M et al. (2022) Biochemically validated structural model of the 15-subunit intraflagellar transport complex IFT-B. EMBO J 41:e112440. https://doi.org/10.15252/embj.2022112440
18. Chlamydomonas Resource Center. https://www.chlamycollection.org/. Accessed 22 May 2025
19. Nievergelt AP, Diener DR, Bogdanova A et al (2024) Protocol for precision editing of endogenous *Chlamydomonas reinhardtii* genes with CRISPR-Cas. STAR Protoc 5:102774. https://doi.org/10.1016/j.xpro.2023.102774
20. Bloodgood RA, Tetreault J, Sloboda RD (2019) The Chlamydomonas flagellar membrane glycoprotein FMG-1B is necessary for expression of force at the flagellar surface. J Cell Sci 132:jcs233429. https://doi.org/10.1242/jcs.233429
21. Dickinson DJ, Schwager F, Pintard L et al (2017) A single-cell biochemistry approach reveals PAR complex dynamics during cell polarization. Dev Cell 42(416–434):e11. https://doi.org/10.1016/j.devcel.2017.07.024
22. Sarıkaya S, Dickinson DJ (2021) Rapid extraction and kinetic analysis of protein complexes from single cells. Biophysical J 120:5018–5031. https://doi.org/10.1016/j.bpj.2021.10.011
23. Zimyanin V, Magaj M, Manzi NI, Yu CH, Gibney T, Chen YZ, Basaran M, Horton X, Siller K, Pani A, Needleman D, Dickinson DJ, Redemann S (2026) Chromokinesin Klp-19 regulates microtubule overlap and dynamics during anaphase in C elegans J Cell Sci 13:jcs.264066. https://doi.org/10.1242/jcs.264066. Epub ahead of print. PMID: 42439517
24. Hutner SH, Provasoli L, Schatz A, Haskins CP (1950) Some approaches to the study of the role of metals in the metabolism of microorganisms. Proc Am Phil Soc 94:152–170
25. Gorman DS, Levine RP (1965) Cytochrome f and plastocyanin: their sequence in the photosynthetic electron transport chain of *Chlamydomonas reinhardi*. Proc Natl Acad Sci 54:1665–1669. https://doi.org/10.1073/pnas.54.6.1665
26. Castoldi M, Popov AV (2003) Purification of brain tubulin through two cycles of polymerization–depolymerization in a high-molarity buffer. Protein Expr Purif 32:83–88. https://doi.org/10.1016/S1046-5928(03)00218-3
27. Hyman A, Drechsel D, Kellogg D et al (1991) Preparation of modified tubulins. Methods Enzymol 196:478–485. https://doi.org/10.1016/0076-6879(91)96041-o
28. Chhatre A (2023) Ex-vivo reconstitution of intraflagellar transport (IFT) train motility. Dissertation, Technische Universität Dresden. https://nbn-resolving.org/urn:nbn:de:bsz:14-qucosa2-900655
29. Schindelin J, Arganda-Carreras I, Frise E et al (2012) Fiji: an open-source platform for biological-image analysis. Nat Methods 9:676–682. https://doi.org/10.1038/nmeth.2019